Carrier tunneling in nanocrystalline silicon–silicon dioxide superlattices: A weak coupling model

B. V. Kamenev,[1] G. F. Grom,[2] D. J. Lockwood,[3] J. P. McCafrey,[3] B. Laikhtman,[4] and L. Tsybeskov[1]
[1]*Department of Electrical and Computer Engineering, New Jersey Institute of Technology, University Heights, Newark, New Jersey 07102, USA*
[2]*Agere Systems, Alhambra, California 91030, USA*
[3]*Institute for Microstructural Sciences, National Research Council, Ottawa, Canada K1A 0R6*
[4]*Racah Institute of Physics, Hebrew University, Jerusalem, Israel*
(Received 15 July 2003; revised manuscript received 8 September 2003; published 8 June 2004)

Differential conductivity measurements in partially disordered nanocrystalline Si–amorphous SiO_2 superlattices reveal a double-peak structure associated with tunneling via energy levels of light and heavy holes. The theoretical model and numerical simulations presented here show good agreement with experiment and predict that this system does not have stable solutions for an injected carrier concentration greater than 10^{17} cm^{-3}. Similar to a weakly coupled superlattice, a larger carrier concentration results in current instabilities. These instabilities have been observed and can be partially suppressed by using pulsed carrier photoinjection.

DOI: 10.1103/PhysRevB.69.235306 PACS number(s): 73.21.Ac, 73.21.La

Attempts to develop a system of coupled nanoscale objects in one, two, or three dimensions have attracted considerable attention recently due to their predicted unique physical properties and wide range of potential applications.[1–6] This task in group IV semiconductors, specifically for Si, is quite complex because of the absence of matching materials for the construction of a high-quality heterostructure. Controlled growth of Si/SiO_2 quantum structures is even more complicated due to the physical nature of the materials [crystalline Si (*c*-Si) and amorphous SiO_2 (*a*-SiO_2)] and the difference in their thermal-expansion properties. Nevertheless, the high quality of the Si/SiO_2 interface and the large potential barriers of Si/SiO_2 could be utilized in systems with efficient carrier confinement and for novel quantum device development. It has been demonstrated previously that a periodic structure consisting of layers of Si nanocrystals separated by *a*-SiO_2 layers possesses abrupt and nearly-defect-free interfaces.[7] The observations of acoustic phonon Brillouin-zone folding[8] and a preliminary indication of the resonant nature in carrier tunneling in these structures[9] have suggested that nanocrystalline (nc-Si)/*a*-SiO_2 superlattices (SL's) can be used in electron quantum devices. These results are surprising, because so far only epitaxially grown semiconductor superlattices have consistently demonstrated such phenomena as resonant carrier tunneling via quantized energy levels, the formation of high-electric-field domains, and the generation of sustained current oscillations.[10] Here we show that sequential resonant tunneling via quantized energy levels and related phenomena can be *quantitatively modeled* in partially disordered nc-Si/*a*-SiO_2 SL's with the assumption of sequential carrier resonant tunneling. Our numerical simulations show that at carrier concentration higher than 10^{17} cm^{-3} this process may lead to the formation of electric-field domains and sustained current oscillations. These simulations together with experiments demonstrate that pulsed carrier injection can suppress the current instabilities. The results reported here demonstrate that partially disordered nc-Si/*a*-SiO_2 SL's exhibit phenomena similar to that observed previously in epitaxially grown weakly coupled superlattices[10] and indicate considerable promise for their device applications.

The nc-Si/*a*-SiO_2 SL's were prepared by the technique of controlled solid-phase crystallization, as described in Ref. 7–9. This nc-Si and *a*-SiO_2 layers were deposited onto an *n*-type 10 kΩ cm *c*-Si substrate, forming an eight period SL with Si nanocrystals of an elliptical shape measuring 4 and 6 nm in the vertical and lateral dimensions, respectively. These layers of Si nanocrystals were separated by 2-nm-thick SiO_2 spacers (extracted from transmission electron microscopy data, not shown). A top Al contact with an area of ~ 1 mm^2 was defined and fabricated using photolithography and wet etching techniques.

To achieve precise control over broad range of carrier concentrations at low temperature, the fabricated structures were illuminated by low-power ($\ll 1$ mW) cw radiation from a He-Ne laser ($\lambda = 632.8$ nm). Since the absorption coefficient in *c*-Si at that wavelength is $\sim 10^4$ cm^{-1} and the entire superlattice is only 52-nm thick, the radiation is totally absorbed in the *c*-Si substrate. Under these experimental conditions, photogenerated carriers are subsequently collected in the substrate or accumulated in the substrate depletion region near the *c*-Si/SiO_2 interface, depending on the sign of the applied bias. Therefore, the experimental conditions can be modeled as carrier injection from a substrate and, depending on the sign of the applied bias, may provide hole or electron injection. Here, only experimental results related to hole transport will be discussed. Differential photoconductance as a function of the applied bias was measured as a low-signal ac conductivity using an ac signal of 10 mV at 88 Hz superimposed on the slowly varying (10 mV/s) dc voltage. The measurements were performed at $T \approx 10$ K.

Differential photoconductivity in a nc-Si/*a*-SiO_2 SL as a function of the applied bias is shown in Fig. 1 for various intensities of the incident laser beam. At the lowest level of excitation (100 μW cm^{-2}), two well-separated peaks are clearly observed in the differential conductivity, with almost an order of magnitude ratio between their maximum and minimum. As the intensity of laser excitation increases, the

 ©2004 The American Physical Society

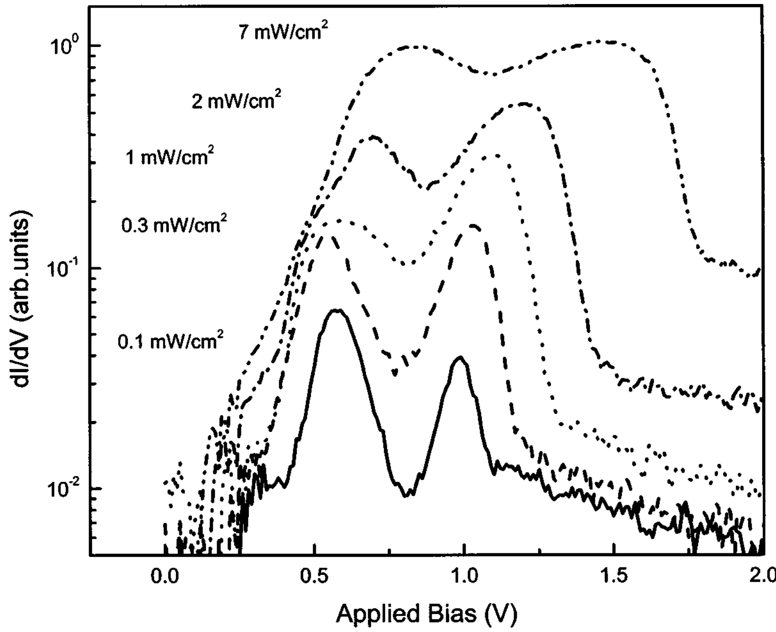

FIG. 1. Differential photoconductivity at T =10 K as a function of the external bias under different levels of 632.8-nm excitation.

peak full width at half maximum (FWHM) increases, peaks shift to higher voltage, and the ratio between the maximum and minimum decreases.

Since the experimental conditions are chosen to provide a monopolar hole injection from the c-Si substrate into the nc-Si/a-SiO_2 SL, we attribute the two peaks to hole tunneling via energy levels of heavy (HH) and light (LH) holes. Our choice is motivated by earlier calcultions, which indicated that the HH2 energy level is higher than the LH1 energy level.[11,12] In conventional superlattices, tunneling from the HH level to the LH level is not very efficient because of spin conservation in pure vertical carrier transport. However, this selection rule is not so strong here due to the LH-HH hole mixing for nonzero in-plane momentum and the possible lateral carrier transport component in nc-Si/a-SiO_2 SL's.[13] An additional perturbation of the wave-function symmetry due to the applied electric field must also be taken into account. Therefore, in a simplified model of sequential tunneling, the first peak in the photoconductance dependence on the applied dc bias may be associated with HH-HH tunneling and the second peak with HH-LH tunneling. The model is illustrated in Fig. 2, where after tunneling to the LH level (1) carriers relax down to the HH level (2).

This process of carrier relaxation and tunneling is not fast and requires a sufficiently long residence time for the charge carrier within a quasi well before the next tunneling event occurs. Our model is consistent with the anticipated extremely low vertical carrier mobility in nc-S/SiO_2 SL's due to a weak coupling between the adjacent Si nanocrystals: the observed sample time constant $\tau=RC$ varies, depending on the excitation conditions, from 1 to 100 ms. Therefore, our assumption of the carrier tunneling process comprising sequences of tunneling/relaxation/tunneling is a reasonable one.

A more complete model needs to include the carrier tunneling dependence on the gradient of the hole concentration and the electric-field distribution across the nc-Si/a-SiO_2 SL. The presence of carriers in the layers of Si nanocrystals induces a redistribution of the applied electric field over the entire SL. This process is responsible for a local modification of the resonance conditions between the adjacent wells in different parts of the SL, tuning the system in and out of the resonance [Fig. 2]. To model the electric-field distribution in a nc-Si/a-SiO_2 SL, the balance equations for the carrier concentration in each layer of Si nanocrystals and the Poisson equation have to be solved self-consistently. This equation system can be written as

$$\frac{\partial p_1}{\partial t} = p_s T_{\rm in} - p_1 T_1 - p_1 T_{\rm in} + p_2 T_1,$$

$$\frac{\partial p_2}{\partial t} = p_1 T_1 - p_2 T_2 - p_2 T_1 + p_3 T_2,$$

$$\vdots \tag{1}$$

$$\frac{\partial p_n}{\partial t} = p_{n-1} T_{n-1} - p_n T_{\rm out} - p_n T_{n-1},$$

$$\xi_{n+1} = \xi_n + \frac{e}{\varepsilon} p_n d_{B,}$$

$$\xi_n = -\frac{\varphi_{n+1} - \varphi_n}{d_{\rm SL}} \tag{2}$$

with the following boundary condition:

$$\Sigma \varphi_n + \varphi_k = V \tag{3}$$

Here p_s is the hole concentration in the substrate, p_n is the hole concentration in the nth well, ξ_n and φ_n are the electric field and potential drop in the nth well, d_B and d_{SL} are the thicknesses of the dioxide barrier and quantum well, T_n is the tunneling coefficient between nth and $(n+1)$th wells, e is the free-electron charge, ε is the dielectric constant, V is the external bias, and $T_{\rm in}$, $T_{\rm out}$ are the SL in and out contact

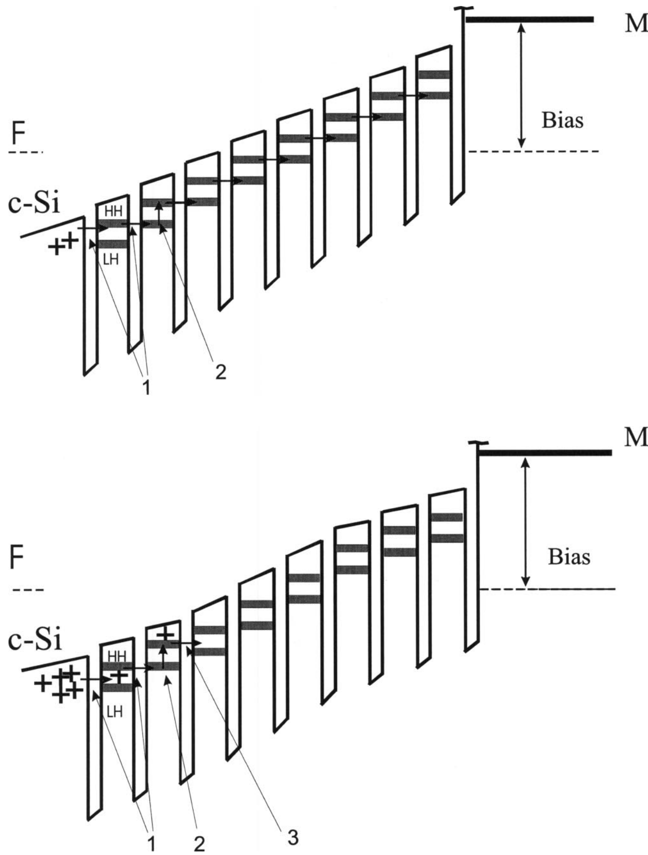

FIG. 2. Valence-band energy diagrams of a SL with (a) homogeneous and (b) nonhomogeneous electric-field distributions. The indicated processes are (1) resonance tunneling of holes via energy levels of heavy (HH) and light (LH) holes; (2) relaxation of holes from LH down to HH levels; (3) destroyed resonance conditions in a SL with a high carrier concentration. *F* and *M* denote the Fermi level of the *c*-Si substrate and metal contact, respectively.

tunneling coefficients, respectively. The first and third terms are the rates between the *n*th and $(n+1)$th well, while the second and fourth are between the *n*th and $(n+1)$th well.

The energy barriers (nc-Si/a-SiO$_2$) between adjacent quasiwells (Si nanocrystals) are very high and the energy dependence of the tunneling coefficients T_n comes mainly from the density of states in the quasiwells. A dispersion of nc-Si sizes and inhomogeneous broadening of the density of states is modeled by a Gaussian function. The tunneling coefficient T_n depends on the potential drop φ_n across the *n*th barrier as

$$T_n \sim A^{h\text{-}h} e^{-(-e\varphi_n/\delta E^h)^2} + A^{h\text{-}l} e^{-[(\Delta E - e\varphi_n)/\delta E^l]^2}, \qquad (4)$$

where $A^{h\text{-}h}$ and $A^{h\text{-}l}$ describe tunneling between HH and LH energy levels, respectively, and contain the corresponding tunneling matrix element squared; δE^h, δE^l are the widths of the heavy and light hole Gaussian-shape density of states; and ΔE is the separation between light and heavy hole energy levels. In our numerical simulations, δE^h, δE^l, and ΔE are used as adjustable parameters. It is significant that the values of δE^h, δE^l obtained from our calculation are $\sim$20 meV. Simple estimations using different methods[14,15] show that for a Si nanocrystal diameter of $\sim$4 nm an energy dispersion of $\sim$20 meV corresponds to $<$10% dispersion in the Si nanocrystal vertical dimension. An additional contribution is expected from small variations in Si nanocrystal shape and crystallographic orientation.

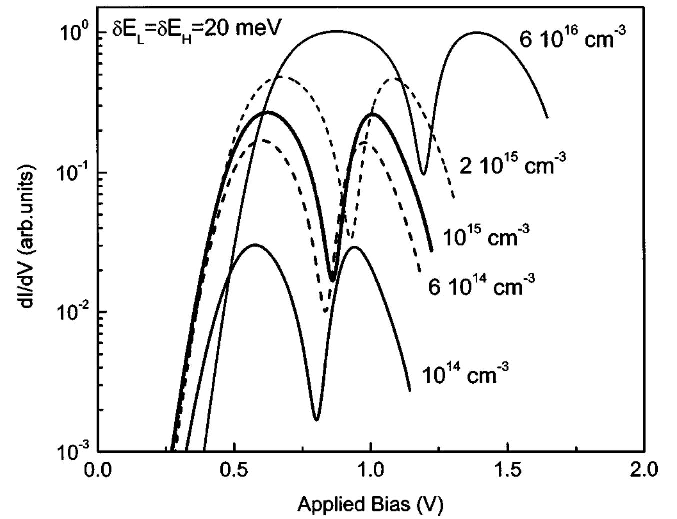

FIG. 3. The calculated dependencies of differential photoconductivity as a function of the external bias for different levels of carrier concentrations.

Coefficients $A^{h\text{-}h}$ and $A^{h\text{-}l}$ are estimated from a simple relationship for tunneling through a square potential barrier,

$$T = \frac{\hbar}{m_{\rm SL}^* d_{\rm SL}^2} e^{-2d_B\sqrt{2m_B^* U/\hbar}}, \qquad (5)$$

where $\hbar$ is the Planck constant, $m_{\rm SL}^*$ and m_B^* are the effective masses of holes in the nc-Si quantum well and SiO$_2$ barrier, and U is the barrier height.

Results of our numerical simulations are shown in Fig. 3. In accordance with our experiment (Fig. 1), the increase in carrier concentration results in an increase of the FWHM in differential conductivity peaks, a decrease in their peak-to-valley ratio, and shift to a higher voltage. More importantly, our simulations predict that the system of Eqs. (1)–(4) with the chosen boundary conditions does not have a stable solution for an injected carrier density into the silicon substrate (i.e., injecting contact) $>10^{17}$ cm^{-3}. What happens when the carrier concentration exceeds 10^{17} cm^{-3}? Figure 4 shows the experimentally observed sustained current oscillations under a much greater cw laser excitation intensity of 100 mW cm^{-2}. By varying the carrier concentration and the applied bias, the oscillation time domain can be changed from milliseconds to hundreds of nanoseconds, most likely due to limitations in the sample *RC*.

A quantitative understanding of carrier tunneling in nc-Si/a-SiO$_2$ SL's can immediately be applied to resolve a long-standing issue concerning the demonstration of NDC in Si-based nanostructures. Since the first reported observation of resonant tunneling and NDC in semiconductor SL's by Esaki *et al.*,[16,17] the importance of a uniform electric field applied across a SL has been pointed out and is well understood. Our simulations show that in order to achieve such a

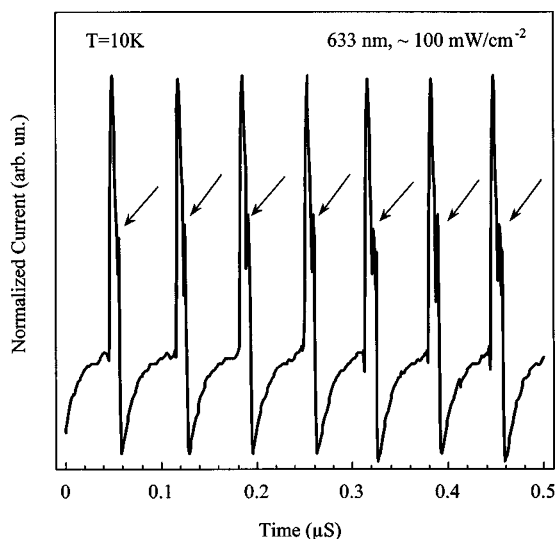

FIG. 4. Experimentally observed current instabilities and sustained oscillations under a cw photoexcitation of $\sim$100 mW/cm^2. Arrows show faster, unresolved components of the oscillations.

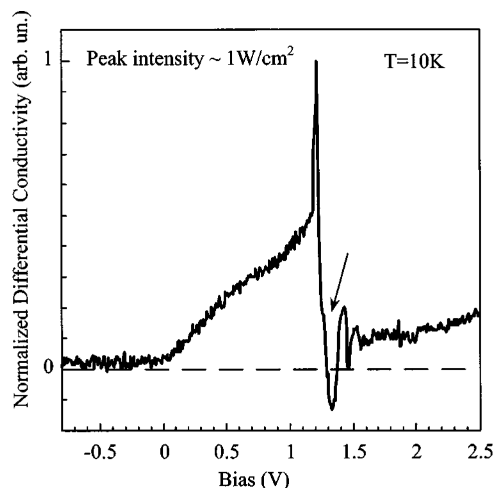

FIG. 5. Differential photoconductivity as a function of the external bias under pulsed photexcitation with a duration of $\sim$10 ms and a peak intensity of $\sim$1 W/cm^2. The pulses are provided by modulation of a cw He-Ne laser beam with a duty cycle of 1:10. The arrows shows the NDC at $\sim$1.3 V followed by the partially suppressed instabilities.

uniform field, the carrier concentration in a nc-Si/SiO_2 SL should be as low as possible. Partial screening of the applied electric field by carriers localized within nc-Si quasiwells destroys the tunneling resonances. However, an effective carrier injection can be produced by a relatively short pulse of light, mostly absorbed in the substrate. At a fixed applied bias, carriers (holes) accumulate at the substrate/SL interface and are entirely immobile until the resonant tunneling conditions occur. When resonance is achieved, carrier mobility increases dramatically and the peak photocurrent as a function of the applied bias may show more pronounced features. A similar technique of transient carrier injection has been applied to study carrier transport in weakly coupled III-V semiconductor superlattices.[18,19] Here this technique is used to detect differential photoconductance under chopped photoexcitation with a low duty cycle. Figure 5 show results of experiments with 632.8-nm excitation at a peak intensity of 1 W cm^{-2} and a duty cycle of $\sim 1:10$. (Note that under the chosen excitation conditions, the pulse duration of 1–10 ms is less than the relaxation time $\tau = RC$.) As a result, a very sharp peak and NDC are observed, indicating that the screening of the applied electric field is less significant. The shape of the photoconductance as a function of the applied bias and the remnant of instabilities indicate that the system is not completely stable.

In conclusion, the observed double-peak feature in photoconductance of nc-Si/a-SiO_2 SL's is attributed to hole sequential resonant tunneling and quantitatively modeled taking into account a nonuniform distribution of the applied electric field due to screening by photogenerated carriers. As an extreme case, this process generates current instabilities and sustained oscillations, similar to phenomena observed previously in epitaxially grwon III-V superlattices. These instabilities can be partially suppressed using pulsed photoinjection of carriers, and thus a better peak-to-valley ratio can be achieved at higher carrier densities. The demonstrated quantitative understanding of carrier resonant tunneling in partially disordered Si nanostructures now permits quantitative modeling and construction of practical electron devices.

This work was supported by Semiconductor Research Corporation, NSF, ARO, Motorola, AMD, and Foundation at NJIT.

[1] L. J. Lauhon, M. S. Gudiksen, D. Wang, and C. M. Lieber, Nature (London) **420**, 57 (2002).
[2] B. A. Korgel, Phys. Rev. Lett. **86**, 127 (2001).
[3] T. M. Wallis, N. Nilius, and W. Ho, Phys. Rev. Lett. **89**, 236802 (2002).
[4] S. Sun and C. B. Murray, J. Appl. Phys. **85**, 4325 (1999).
[5] A. J. Williamson, J. C. Grossman, R. Q. Hood, A. Puzder, and G. Galli, Phys. Rev. Lett. **89**, 196803 (2002).
[6] S. A. Crooker, J. A. Hollingsworth, S. Tretiak, and V. I. Klimov, Phys. Rev. Lett. **89**, 186802 (2002).
[7] L. Tsybeskov, K. D. Hirschman, S. P. Duttagupta, M. Zacharias, P. M. Fauchet, J. P. McCaffrey, and D. J. Lockwood, Appl. Phys. Lett. **72**, 43 (1998).
[8] G. F. Grom, D. J. Lockwood, J. P. McCaffrey, H. J. Labbe, L. Tsybeskov, P. M. Fauchet, B. White, J. Diener, H. Heckler, D. Kovalev, and F. Koch, Nature (London) **407**, 358 (2000).
[9] L. Tsybeskov, G. F. Grom, R. Krishnan, L. Montes, P. M. Fauchet, D. Kovalev, J. Diener, V. Timoshenko, F. Koch, J. P. McCaffrey, H. J. Labbe, G. I. Sproule, D. J. Lockwood, Y. M. Niquet, C. Delerue, and G. Allan, Europhys. Lett. **55**, 552

(2001).
[10] See, for example, *Semiconductor Superlattices: Growth and Electronic Properties*, edited by H. T. Grahm (World Scientific, Singapore, 1995), p. 250.
[11] A. V. Chaplik and L. D. Shvartsman, Phys. Chem. Mech. Surf. **2**, 73 (1982).
[12] B. Laikhtman, R. A. Kiehl, and D. J. Frank, J. Appl. Phys. **70**, 1531 (1991).
[13] D. L. Miller and B. Laikhtman, Phys. Rev. B **54**, 10 669 (1996).
[14] C. Delerue, M. Lannoo, and G. Allan, Phys. Rev. Lett. **84**, 2457 (2000).
[15] S. Ögüt, J. R. Chelikowsky, and S. G. Louie, Phys. Rev. Lett. **79**, 1770 (1997).
[16] L. Esaki and L. L. Chang, Phys. Rev. Lett. **33**, 495 (1974).
[17] R. Tsu, L. L. Chang, G. A. Sai-Halasz, and L. Esaki, Phys. Rev. Lett. **34**, 1509 (1975).
[18] S. Tarucha, K. Ploog, and K. von Klitzing, Phys. Rev. B **36**, 4558 (1987).
[19] W. Muller, D. Bertran, H. T. Grahn, K. von Klitzing, and K. Ploog, Phys. Rev. B **50**, 10 998 (1994).